Projekt zum Fortgeschrittenen-Praktikum - Atomic Force Microscopy

Guilherme Stein & Ulrich Müller

Supervisor: Dr. Paolo Sessi

Date of experiment: 4th October 2013

1 Expose

The III-V semiconductor system based on GaSb is commonly used for optical semiconductor devices with wavelengths beyond 2.3 µm [1]. In Würzburg especially the interband cascade lasers, which are grown by MBE on GaSb substrate, made significant progress during the last years [2]. In order to grow devices with high performance it is inevitable to use high quality substrates with a minimum of defects. Despite the use of 'epi-ready' substrates the wafers suffer from native oxide like Ga_2O_3 and Sb_2O_3 [3]. The growth of devices on top of this oxide would lead to non-monocrystal layers. To remove this oxide a commonly used technique in Würzburg is to heat the substrate to about 580° for a short time. At this temperature the most of the oxide desorbes from the surface but leaving holes in the surface with about 10 nm in size [4]. Hereupon a 200 nm GaSb buffer layer is grown at 485° to flatten the surface.
This method has been established during the last years although it is not clear whether a different technique would lead to smoother surfaces. Therefore one of the goals of this experiment is to determine a method of reducing the roughness on the wafer we want to grow on optical structures. This is important on the behalf of the optical quality the device can operate at.

From an intuitive point of view it is clear what roughness is. However, quantifying roughness in a mathematical way is not trivial. Common definitions use the standard deviation of the surface's mean height as $S_a = \frac{1}{A}\iint_A |z(x,y)|\mathrm{d}x\mathrm{d}y$ and are suitable in many applications. Problems arise when applying this definition to non-flat surfaces. A soup bowl which appears flat and smooth when we are very close to the surface, shows a curvature when we look at the object as a whole. This example shows, that roughness is not independent of the scale. In our scope roughness will be a way of measuring the quality of a surface with respect to certain properties of the material. We think that in general the concept of a surface energy is a better approach to address the optical properties arising from surface irregularities. The more the size of the surface differs from a perfect flat surface the rougher the surface is. We want to model the surface as polygons connecting the mean heights of a discrete lattice. The lattice size represents the scaling parameter mentioned above. Here we make the arbitrary choice of the AFM's resolution which will be the scale on which we measure the roughness of the samples.

The Atomic Force Microscope (AFM) is the perfect instrument to characterize this roughness of the wafers as it determines the height of the surface very precisely. The expected differences in height on the surface is about 10 nm which is within the resolution of the AFM. As the AFM doesn't work in situ we have to produce and investigate the surface at each step of the growth process to understand the mechanisms of oxide desorbtion and flattening of the surface. We are going to characterize the single steps of the standard process which are: an untreated GaSb wafer, the wafer after the oxide desorbtion and after the growth of 200 nm GaSb buffer. To vary this process we want to test two aspects: first the increase of the GaSb buffer's growth temperature up to 500° and 515° and second the growth of a 30 nm GaSb/AlAsSb superlattice directly after oxide desorbtion. Recent research showed that the growth of

Figure 1: At the sample's surface after several micrometer growth small pyramidal defects are visible. The image was taken by an optical microscope at a magnification of 50.

AlAsSb shutting down the step-flow growth mode. This step-flow growth mode is dominant during the growth of GaSb layers and is not very successful in flattening bigger defects like defects in pyramidal shape [4]. The growth of a superlattice instead of a bulk layer is nevertheless necessary to maintain the electrical conductivity of the sample. It would be helpful to understand how these defects can be removed from the surface and how the process can be improved. If the smoothing is not successful theses pyramidal defects tend to grow bigger as the growth progresses. After the growth of structures with a thickness of several microns these defects can even be observed by a optical microscope as shown in figure 1.

After sample production exposure to air can not be avoided. To reduce surface corrosion the samples will be produced tight before the experiment and stored in a nitrogen-flooded cabinet.

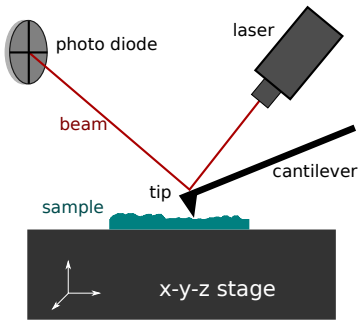

Figure 2: Simplified illustration of an atomic force microscope

2 Basics

The relevance of fabrication and therefore also the analysis of structure in the sub-micrometer and even nanometer scale has increased steadily in the past decades. In contrast to other scanning imaging techniques as the STM or SEM, the atomic force microscope (AFM) is capable to deliver up to atomic resolution without the need of a vacuum or special treatment of the probe prior to analysis. This allows us to examine a broader variety of samples under easily achievable conditions.

2.1 Work principle of the AFM

The principle of the atomic force microscope are the forces that act between two pieces of matter when brought close to each other. More precisely we bring a sharp tip into a distance of a few nano meters to a surface we want to examine. scale the main contribution are Van-der-Waals forces which arise from polarisation fluctuations in the material. In figure 2 one can see the main parts required to run the AFM. The sample is mounted on a xyz-stage consisting of different piezo elements. This enables us to move the sample in xy-direction for the scanning of the probe, as well as in the z direction for height compensation. A reflecting cantilever is positioned above the sample. A laser beam will reflect on the cantilever and hits a segmented photodiode. If the cantilever moves, the laser beam will change the angle of deflection, detectable by the photodiode. From the intensity change on the diode segments one can calculate the height difference of the material.

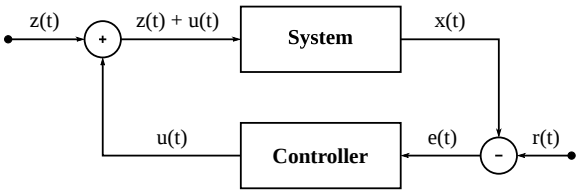

Figure 3: Principle of a feedback loop with disturbance $z(t)$, output $r(t)$, control signal $u(t)$, measured output $x(t)$ and error signal $e(t)$.

2.2 Refinements

Instead of mapping the intensity change on the diode to the force and subsequently to the probe height, often a different approach is used. The tip is set to apply a constant force on the probe. If the force changes, the piezo in z-direction is altered to move the probe to a height where the force is equal to the set point defined before. This has the advantage that the force between tip and probe is approximately constant and therefore it is less likely to damage the sample or the tip. This is ensured via a feedback loop between the the diode and the piezo element as seen in figure 3.

The height information accquired via this method is more strongly connected to the actual sample surface. The mapping is done between the piezo voltage as opposed to the strength of the diode, the angle of the lase beam and the distances between those elements. Therefore introducing less error sources and leading to a more accurate signal.

Relevanz für die Aufnahme der GaSb Proben

3 Data Aquisition

3.1 Parameter of recording

In order to acquire the topology of the samples surface the computer records the scanner's z-position in combination with the in plane x- and y-position. These data can be exported from the control software in a special (.ezd) data format. We convert these data back into a list of x, y and z-coordinates using the *WSxM* software, which is freely available on ??.

While scanning in static force mode is necessary to maintain the force by moving the scanner's z-position. This is done by a feedback loop, which compares the a stated force constant to the force calculated from the signal of the photodiode. The difference is called the error signal and is the basis for the PI-controller. This controller includes to variables, the P- and I-values, which can be adjusted at the control software. While recording the data we can adjust the P- and I-values to optimize the quality of the pictures and avoid image artifacts. These values refer to the proportional and integral gain of the z-controllers feedback loop respectively. The proportional gain provides a signal which is proportional to the error signal. By increasing this value one should observe a smaller static error signal and a faster adaption to the current height position. On the other hand, if this value is set to high, one should observe a overshoots while scanning steps. Even higher P-values lead to more noise as the scanner is reacting oversensitive to little changes in height. The I-value however provides a signal which is proportional to the temporal integral of the error signal. The adaption of this value may have similar effects as adaption the P-value. Nevertheless the signal from the integral controller is lee sensitive to noise.

In the beginning of the experiment we scanned a calibration grid while varying the P- and I-parameter to see the effects on the pictures quality. The calibration grid consists of a grid with two different height levels. By scanning the grid in one direction one should observe steps in the up and down direction. In the following pictures every scan is conducted from the left the right side. Firstly we started with a low I-value and observed the z-coordinate adepting very slowly to the actual height of the grid as is shown in 4a.

By increasing the I-value the height is adapting much more quickly but overshoots at the step's edge as well as increasing the amount of noise during the plateaus. The height profile is plotted in 4b.

In the next step the influence of the P-value was observed. With the I-value set to 9 the p-value was varied from 5 to 15. Interestingly an decrease of the P-value to 5 doesn't change much but increasing the overshoots caused by the I-value, which is set little higher than the optimum value. Simultaneously the overshoots decrease when increasing the P-value. This however has a negative influence on the noise as can be seen in the comparison of 4c and 4d.

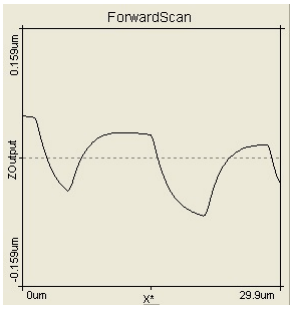

(a) I-gain set to 5. P = 9.

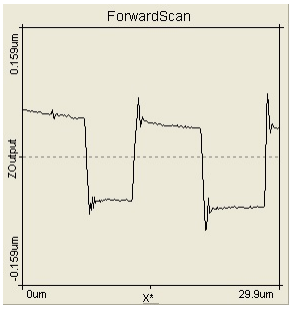

(b) I-gain set to 11. P = 9.

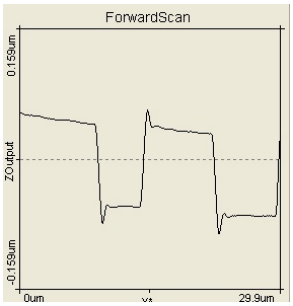

(c) P-gain set to 5. I = 9.

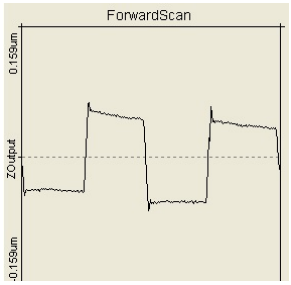

(d) P-gain set to 15. I = 9.

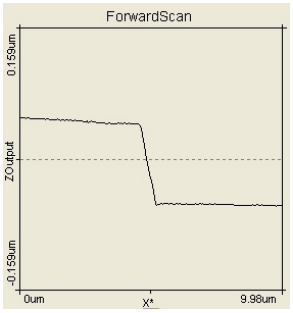

(e) Scanning speed of 3 s per line. P = 9, I = 9.

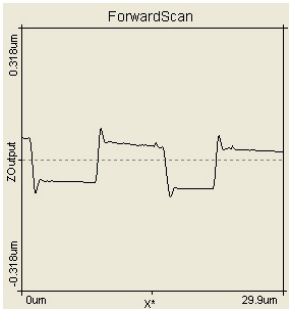

(f) Scanning speed of 0.7 s per line. P = 9, I = 9.

Figure 4: Height profiles of single lines and the effect of different feedback parameters and scanning velocities. Scanning direction is from left to right.

As a trade-off between fast and accurate height adaption and a minimum of noise we choose I = 9 and I = 7. We use these parameters in all following measurements, if not stated differently.

Next we want to investigate what influence the speed of scanning has on the image recording. We measure the calibration grid with 0.7 s and 3 s per line. During this period 256 data points are recorded along the scanning axis. For the slow scan speed we observe in 4e the clear step of the calibration grit without any noticeable overshoot. For the faster scanning speed we can see in 4f distinct overshoots at the beginning of each step.

Although we observe artifacts while scanning the calibration grit with 0.7 s per line it is possible to measure structures without steep gradient with a higher scanning speed without observing overshoots.

3.2 Data preparation

When acquiring data there is always an interpretation and processing involved. This is necessary to make sense of the data, especially when dealing with big data sets. This strongly depends on the uses of the data, i.e. getting a general idea of an object or measuring something with great accuracy to search for yet undiscovered principles. While the unprocessed set has little meaning, we edit it and thereby imprint a meaning into the data. Some may argue this leads to wrong data, or at least reduces the quality. On the other hand, there is no such thing as a perfect measurement. Therefore the data we acquire will never be an exact representation of the object we want to project. We need to make corrections based on our model of the world to increase the quality and, even more crucial, the usefullness of our measurements. It is absolutely necessaty not to accidentally manipulate the data in a unscientific manner. Thus we need to know all the time what has been done with the data and to document the process of analysis. With the AFM we scan a sample with great precision in a rasterized format. Each image consists of discrete coordinates. Our goal is to analyse the samples surface. One step is the removal of systematic errors. If the sample is known to be flat we can make a fit to the underground. While manipulating the data quite a bit, we remove a simple error, i.e. a tilt in the plane known to be something irrelevant for our purpose. In this case even underground fits of higher order might be

useful considering deviations created by nonlinearities of the piezo tube or other elements. On this example we want to show how this is done in detail, when it is legitimate and where problems may occur. In 5 the raw data image from sample ⑦ are plotted.

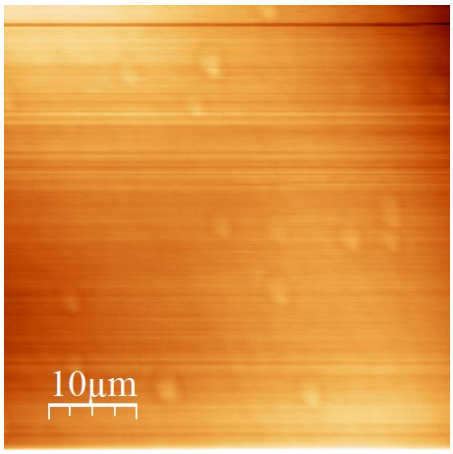

Figure 5: The raw data image from sample ⑦.

We can clearly identify the horizontal direction in which the tip scanned the sample. After each row the tip is afflicted with a different offset leading to different heights/colors for each row. This offset is not a feature of our sample, so we try to manipulate the data in a way to get rid of this effect. In detail this is done by fitting a parabola to each row of our sample, subtracting this parabola from the raw data afterwards. The same method applied on the single column removes the tilt in the y-axis. After applying this flatten function the features of our sample are visible much better and the stripy surface has been manly removed.
As mentioned before every correction falsify the data to a certain amount and the method should not be applied without being aware of the problems which may occur.

In the 7 the surface of ① is showed. Noticeable in the middle of the picture we find a peak on a otherwise flat surface. By applying the flatten function we receive the picture shown in **??**. Horizontally and vertically from the peak a darker cross has emerged. This can be explained in the following way. By fitting over the row/column including the peak the mean height is higher. By subtracting the fitted function from raw data, every row/column including the peak is lowered more than the other ones. This leads to an unwanted artifact near the peak.

In summary we consider the flatten method a a legiti-

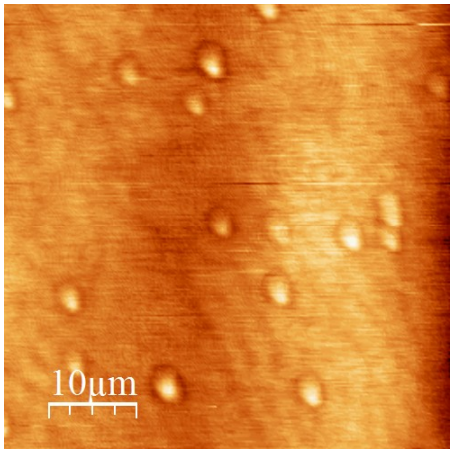

Figure 6: Data of sample ⑦ flattened in row and column.

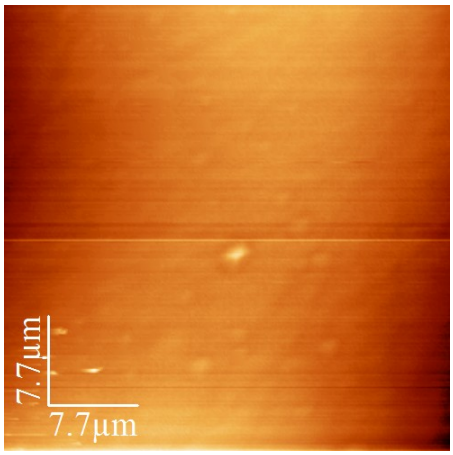

Figure 7: The raw data image from sample ①.

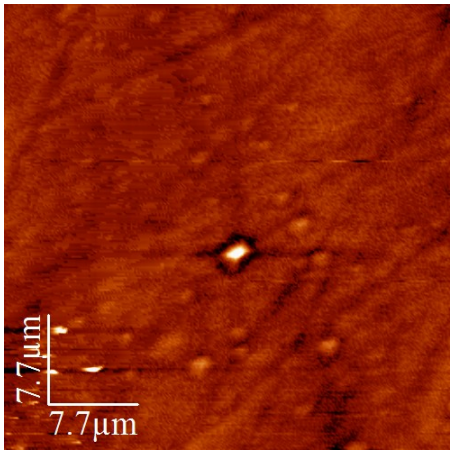

Figure 8: Data of sample ① flattened in row and column. A artifact horizontally and vertically from the peak has emerged.

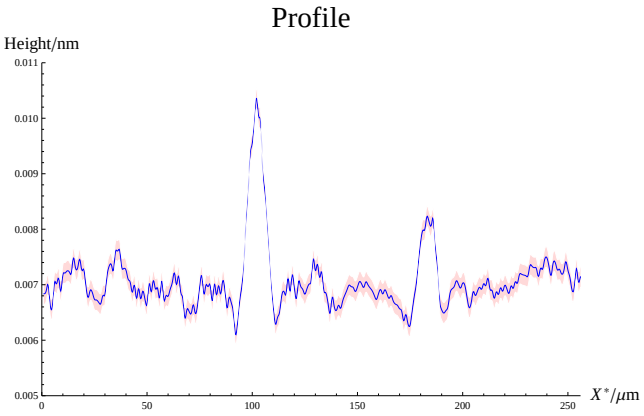

Figure 9: Height profile plotted with an estimation of noise. Two peaks at 100 µm and 185 µm are visible which are much higher than the level of noise.

mate tool for data preparation but one has to be aware of the artifacts which may occur.

3.3 Signal and noise

During the measurements of the calibration grid the amplitudes of the single steps are much higher than the level of noise. While measuring flatter surfaces this in not the case however. During the measurement of sample (?) we observed features which are in order of 4 nm. Here it becomes more and more important to quantify the amount of noise to distinguish between real features and random noise. From the difference between the forward and backward scans we can estimate the amount of noise comprised in our data: First we take the data points from one line, forward and backward, and shift them to a maximum overlap. Secondly we calculate the difference between these two scans. From these aberrations we receive a standard deviation between the two scans. Dividing by $\sqrt{2}$ provides the standard deviation of the measurement. As an example in figure 9 the signal and an area with the size of the measurement's standard deviation is plotted. The signal is calculated by the mean value of the forward and backward scan.

Therefore we can say that the peaks at 100 µm and 185 µm are real features while there is no significance for the peaks beyond 200 µm.

Additionally to the noise we observe artifacts which can be clearly identified as they only appear in one, either forward or backward direction. One artifact we want to discuss is shown in figure 10. In one single line we can

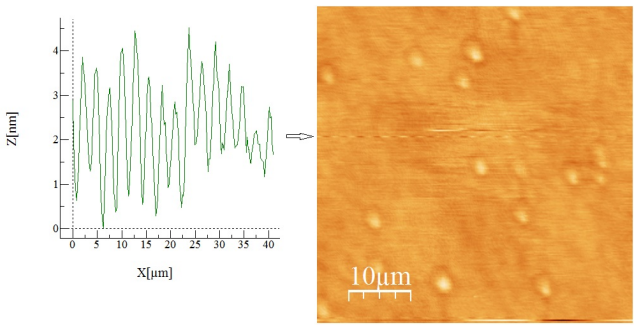

Figure 10: Height profile plotted with an estimation of noise. Two peaks at 100 µm and 185 µm are visible which are much higher than the level of noise.

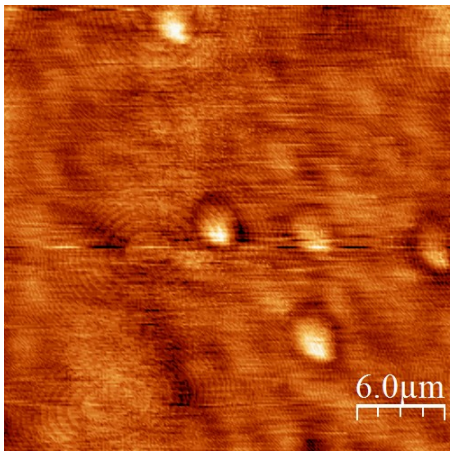

Figure 11: Oval pattern.

see a periodic pattern which is shown in 10. The the periodicity of this artifact is approximately 2.5 µm but we find oscillations with an other periodicity as well. ??Why

Furthermore we found pattern which looks like concentric sets of ovals. The distance between two ovals decreases as their size increases. We find these elliptic pattern in every of our GaSb samples. One surface with clearly visible patterns is shown in 11. ??Why

M ethoden und Probleme der Bildbearbeitung

4 Sample Analysis

- Features

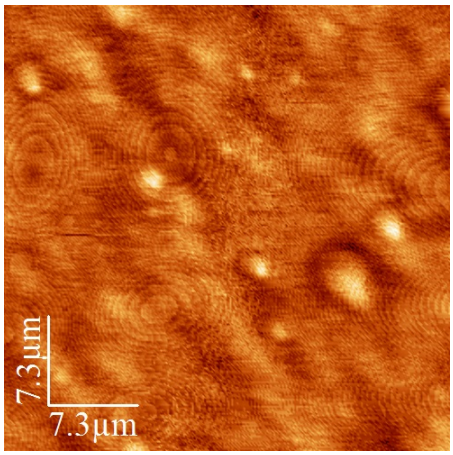

Figure 12: Oval pattern.

- Linien unterschiedlich
- einzelne hohe Punkte mit Graben außenherum
- Rauigkeit der Oberfläche
- Aussagen über Wachstumsmethoden

References

[1] Shamsul Arafin (2012): Electrically-Pumped GaSb-Based Vertical-Cavity Surface-Emitting Lasers. München.

[2] Weih, Robert; Kamp, Martin; Höfling, Sven (2013): Interband cascade lasers with room temperature threshold current densities below 100 A/cm2. In: Appl. Phys. Lett. 102 (23), S. 231123. DOI: 10.1063/1.4811133.

[3] C.J. Vineis; C.A. Wang; K.F. Jensen (2001): In-situ reflectance monitoring of GaSb substrate oxide desorption 2001.

[4] Murray, Lee M.; Yildirim, Asli; Provence, Sydney R.; Norton, Dennis T.; Boggess, Thomas F.; Prineas, John P. (2013): Causes and elimination of pyramidal defects in GaSb-based epitaxial layers. In: J. Vac. Sci. Technol. B 31 (3), S. 03C108. DOI: 10.1116/1.4792515.

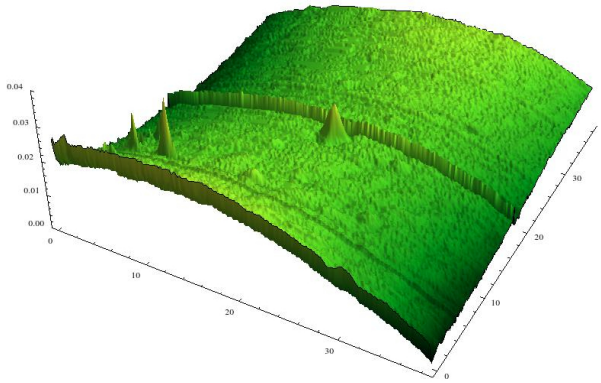

(a) Sample ① : GaSb grown at 485°C, original scan.

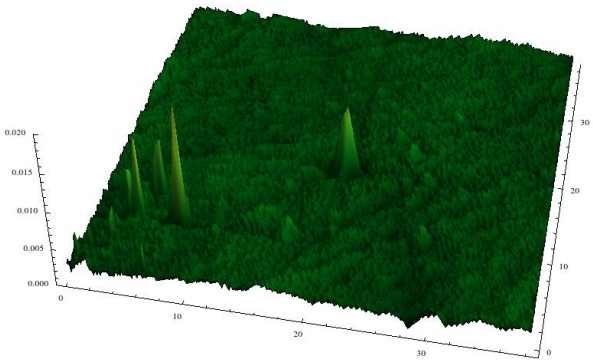

(b) Sample ① : GaSb grown at 485°C, flat.

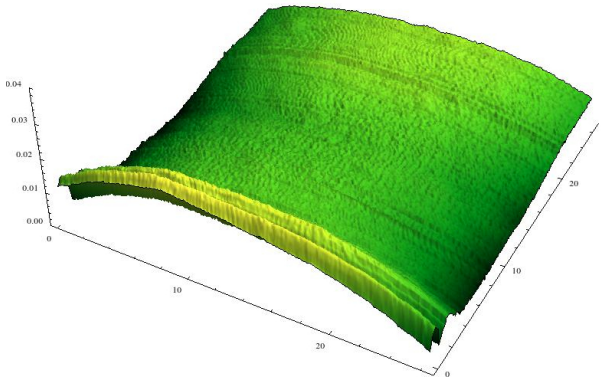

(c) Sample ② : GaSb grown at 515°C, original scan.

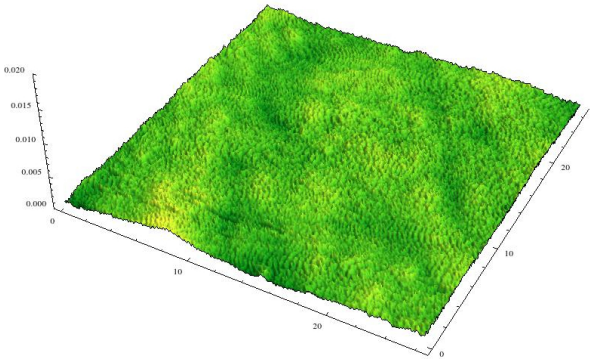

(d) Sample ② : GaSb grown at 515°C, flat.

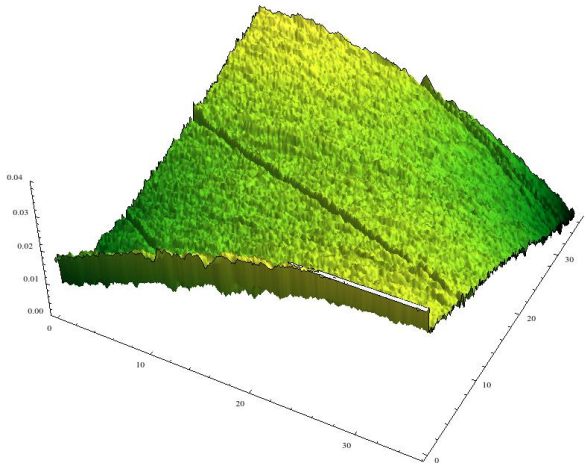

(e) Sample ③ : GaSb untreated wafer, original scan.

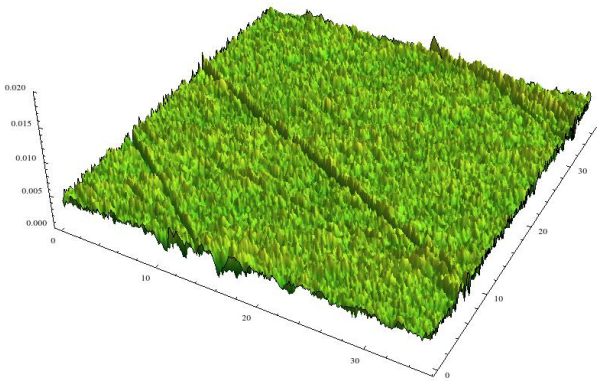

(f) Sample ③ : GaSb untreated wafer, flat.

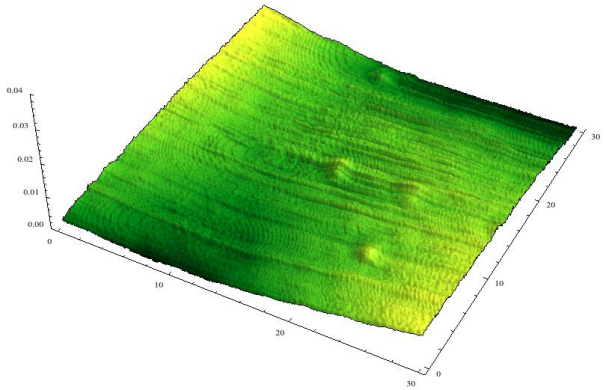

(g) Sample ④ : Al grown on wafer, original scan.

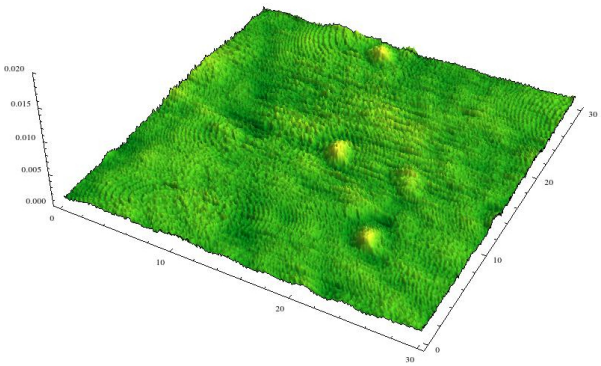

(h) Sample ④ : Al grown on wafer, flat.

Figure 13: Comparison of samples analyzed in the experiment. In the flat plots we subtracted a linewise fitted quadratic function from the original scan data